Eur. J. Biochem. **270**, 1076–1088 (2003) © FEBS 2003 doi:10.1046/j.1432-1033.2003.03435.x

Human acid sphingomyelinase
Assignment of the disulfide bond pattern

Stephanie Lansmann[1], Christina G. Schuette[2], Oliver Bartelsen[1], Joerg Hoernschemeyer[1], Thomas Linke[1], Judith Weisgerber[1] and Konrad Sandhoff[1]

[1]*Kekulé-Institut für Organische Chemie und Biochemie, Universität Bonn, Germany;*
[2]*Max-Planck-Institut für Biophysikalische Chemie, Göttingen, Germany*

Human acid sphingomyelinase (haSMase, EC 3.1.4.12) catalyzes the lysosomal degradation of sphingomyelin to ceramide and phosphorylcholine. An inherited haSMase deficiency leads to Niemann–Pick disease, a severe sphingolipid storage disorder.

The enzyme was purified and cloned over 10 years ago. Since then, only a few structural properties of haSMase have been elucidated. For understanding of its complex functions including its role in certain signaling and apoptosis events, complete structural information about the enzyme is necessary. Here, the identification of the disulfide bond pattern of haSMase is reported for the first time. Functional recombinant enzyme expressed in SF21 cells using the baculovirus expression system was purified and digested by trypsin. MALDI-MS analysis of the resulting peptides revealed the four disulfide bonds Cys120-Cys131, Cys385-Cys431, Cys584-Cys588 and Cys594-Cys607. Two additional disulfide bonds (Cys221-Cys226 and Cys227-Cys250) which were not directly accessible by tryptic cleavage, were identified by a combination of a method of partial reduction and MALDI-PSD analysis. In the sphingolipid activator protein (SAP)-homologous N-terminal domain of haSMase, one disulfide bond was assigned as Cys120-Cys131. The existence of two additional disulfide bridges in this region was proved, as was expected for the known disulfide bond pattern of SAP-type domains. These results support the hypothesis that haSMase possesses an intramolecular SAP-type activator domain as predicted by sequence comparison [Ponting, C.P. (1994) *Protein Sci.*, **3**, 359–361].

An additional analysis of haSMase isolated from human placenta shows that the recombinant and the native human protein possess an identical disulfide structure.

Keywords: disulfide bonds; enzymatic and chemical cleavage; human acid sphingomyelinase; MALDI-MS; PSD.

Human acid sphingomyelinase (haSMase, EC 3.1.4.12) is a lysosomal enzyme catalyzing the degradation of sphingomyelin (SM), a major lipid constituent of the extracellular side of eukaryotic plasma membranes, to ceramide and phosphorylcholine. Enzyme deficiency due to mutations in the haSMase gene leads to Niemann–Pick disease, an autosomal recessive sphingolipidosis [1]. The infantile type A of Niemann–Pick disease manifests itself in rapid neurodegeneration and patients die within three years, whereas Niemann–Pick disease type B patients suffer from a non-neurological visceral progression of this disorder. For these patients, enzyme replacement would be a possible form of therapy and in fact, a clinical trial is scheduled to start in the near future (http://www.nnpdf.org/typeb/). This development raises an additional interest in information about the structure and the post-translational modifications of the enzyme.

More than 10 years ago the enzyme was purified from urine [2] and the full-length cDNA encoding haSMase was isolated [3,4]. The enzyme was shown to be a monomeric 72 kDa glycoprotein containing a protein core of 61 kDa. The full-length haSMase-cDNA contains an open reading frame of 1890 bp encoding 629 amino acids. Biosynthesis studies in human fibroblasts revealed stepwise proteolytic processing of a 75-kDa haSMase precursor form to the mature protein during transport to the lysosomes [5]. Mature haSMase possesses six potential N-glycosylation sites as was recently shown by N-terminal sequencing [6]. Site-directed mutagenesis of the potential glycosylation sites and subsequent expression of mutated cDNA constructs indicated that at least five of them are used *in vivo* [7].

Ceramide and sphingosine, the products of the SM and ceramide degradation, were recently recognized as lipid modulators and/or second messengers in receptor-mediated signal transduction processes resulting in apoptosis, differentiation and proliferation of different cell types [8,9]. Neutral and acid sphingomyelinase seem to be involved in

Correspondence to K. Sandhoff, Kekulé-Institut für Organische Chemie und Biochemie, Universität Bonn, Gerhard-Domagk-Str. 1, D-53121 Bonn, Germany,
Fax: +49 228737778, Tel.: +49 228735346,
E-mail: sandhoff@uni-bonn.de

Abbreviations: BCA, bicinchoninic acid; bc-haSMase, haSMase expressed in SF21 cells using the baculovirus expression vector system; haSMase, human acid sphingomyelinase; OG, octyl-β-D-glucopyranoside; pl-haSMase, haSMase isolated from human placenta; PNGase F, peptide N-glycanase F; PSD, post source decay; SAP, sphingolipid activator protein; SM, sphingomyelin; [^{3}H]SM, [^{3}H]sphingomyelin, ^{3}H-labeled in the choline moiety; TCEP, tris(2-carboxyethyl)phosphine hydrochloride.

Enzymes: acid sphingomyelinase (EC 3.1.4.12); trypsin (EC 3.4.21.4); peptide *N*-glycanase F (EC 3.5.1.52).

(Received 8 August 2002, revised 4 December 2002, accepted 17 December 2002)

these cell signaling events dependent on the cell type and the respective stimulus [10]. Recent findings indicate that acid sphingomyelinase plays an important role in CD95-induced apoptosis [11].

Several lysosomal sphingolipid hydrolases require sphingolipid activator proteins (SAPs) as cofactors for the *in vivo* degradation of substrates with short hydrophilic headgroups. However, the presence of SAPs is not essential for the *in vivo* degradation of SM by haSMase [12]. Amino acid sequence alignment of SAP-type domains revealed a strong homology between the sequences of SAP A-D and the N-terminal region of haSMase [13]. Most notably, the positions of the six cysteine residues found in all sequences are strictly conserved. The high degree of sequence similarity led to the hypothesis that haSMase possesses its own activator domain for the interaction with the membrane-bound lipid substrate. As recently reported, the disulfide bond structure of SAP B-D is identical for all three proteins [14,15]. Disulfide analysis must show, whether the SAP-homologous domain within haSMase also possesses the SAP-type disulfide structure.

Detailed structural information will be essential for understanding of the complex functions of acid sphingomyelinase including the role of its SAP-homologous domain. The analysis of post-translational modifications such as the disulfide bond pattern and the glycosylation is an important first step toward the structural characterization of haSMase by molecular modeling and X-ray crystallography. In addition, this information may be of importance in the design of an enzyme replacement therapy for Niemann–Pick type B patients. Here, we present for the first time the disulfide bond pattern of haSMase. With respect to the disulfide bridges, recombinant haSMase expressed in SF21 cells using the baculovirus expression system is compared to the native human protein isolated from human placenta.

Experimental procedures

Reagents

Modified trypsin of sequencing grade was obtained from Promega. TCEP was purchased from Pierce. 1-cyano-4-dimethylamino-pyridinium tetrafluoroborate, α-cyano-4-hydroxycinnamic acid, sinapinic acid and standard peptides for MALDI-MS calibration were obtained from Sigma-Aldrich.

MALDI mass spectrometry

MALDI-MS analysis was performed on a TofSpec E mass spectrometer (Micromass, Manchester, UK) with a 337-nm nitrogen laser. The acceleration voltage was set to 20 kV. An extraction voltage of 19.5 kV and a focus voltage of 15.5 kV were used. A pulse voltage of 2200–2400 V was used for measurements in the reflectron mode and of 1200 V for measurements in the linear mode (above 4 kDa). Measurements were performed at threshold laser energy. Post source decay (PSD) was performed as described by the supplier.

Matrix solutions. α-Cyano-4-hydroxycinnamic acid, 10 mg·mL^{-1} in 50% acetonitrile, 50% water containing 0.1% trifluoroacetic acid or sinapinic acid, 10 mg·mL^{-1} in 40% acetonitrile, 60% water containing 0.1% trifluoroacetic acid (high salt concentrations and/or above 4 kDa).

Sample preparation. The peptide solution was mixed with the matrix solution (each 1 μL) on the target and dried at room temperature. Calibration was performed as three or four point external calibration using standard peptides.

Tryptic digestion

Purified bc-haSMase (1.5 mg·mL^{-1}) in 25 mM NH_4HCO_3 containing 0.1% (w/v) octyl-β-D-glucopyranoside (OG) was incubated with modified trypsin in an enzyme : protein ratio of 1 : 20 at 37 °C for 15 h. Digestion was stopped by freezing in liquid N_2.

RP-HPLC separation

Reverse phase-(RP) HPLC separation of peptides was performed on a SMART System (Pharmacia, Uppsala, Sweden) using a Nucleosil C18 column (3 μm particle size, 120 Å pore, 2 × 250 mm) at a flow rate of 100 μL·min^{-1}.

Tryptic peptides. Trifluoroacetic acid (0.1%) in water was used as solvent A and 0.06% trifluoroacetic acid in 70% acetonitrile and 30% isopropanol as solvent B. The C18 column was equilibrated in 5% B. Sample injection was followed by washing with 5% B for 20 min and peptides were eluted with a linear gradient of 15% to 60% B in 80 min.

Singly reduced peptides. Trifluoroacetic acid (0.1%) in water was used as solvent A and 0.08% trifluoroacetic acid in 80% acetonitrile and 20% water as solvent B. The C18 column was equilibrated in 30% B. After sample injection and washing with 30% B for 20 min the partially reduced peptides were eluted using a linear gradient of 30% to 70% B in 60 min.

Disulfide bond and glycosylation analysis

The peptides of the tryptic digest were separated by RP-HPLC. After adding 0.04% (w/v) OG, the fractions were concentrated (≈ 20 μM) at room temperature in a vacuum centrifuge and subjected to MALDI-MS analysis.

Disulfide bonds. Aliquots of fractions containing disulfide-linked peptides were lyophilized and redissolved in 25 mM NH_4HCO_3 (≈ 20 μM). The samples were analyzed by MALDI-MS without prior treatment, after reduction with tris(2-carboxyethyl)phosphine hydrochloride (TCEP; 2 mM, 37 °C, 1 h), and after subsequent alkylation with iodacetamide (5 mM, 30 min) in the dark at room temperature.

Glycosylation. Lyophilized aliquots of fractions containing glycopeptides were redissolved in 25 mM NH_4HCO_3 (≈ 20 μM). Before and after treatment with peptide N-glycanase F (PNGase F; 100 U) at 37 °C for 3 h, the samples were analyzed by MALDI-MS.

Partial reduction, cyanylation and fragmentation

Partial reduction of peptide T14 + T17. Isolated disulfide-linked peptide T14 + T17 (3 nmol) was lyophilized and redissolved in 16 μL 0.1 M citrate buffer (pH 3) containing 6 M guanidine-HCl and 20 μL of 0.1 M citrate buffer (pH 3) were added. For the partial reduction of peptide disulfide bonds, 4 μL of 20 mM TCEP in 0.1 M citrate buffer (pH 3) were added and the mixture was incubated at room temperature for 10 min.

Cyanylation of nascent sulfhydryls. After adding 10 μL of 0.1 M 1-cyano-4-dimethylamino-pyridinium tetrafluoroborate in 0.1 M citrate buffer (pH 3), the mixture was incubated at room temperature for 10 min to cyanylate nascent sulfhydryls. The reaction was stopped by freezing or by adding 0.1% trifluoroacetic acid.

Cleavage of cyanylated peptides. Cyanylated peptides were separated by RP-HPLC, 0.04% (w/v) OG was added to each fraction and the organic solvent was removed in a vacuum centrifuge. The lyophilized peptides were redissolved in 2 μL of 6 M guanidine-HCl in 1 M NH_4OH and 6 μL of 1 M NH_4OH were added. Cleavage of the peptide chain was performed at room temperature for 1 h. Excess ammonia was removed in a vacuum system. The dried peptide fragments were redissolved in 20 μL of 10 mM NH_4HCO_3.

Reduction of the remaining disulfide bonds. Cleaved peptides, still linked by a residual disulfide bond were treated with 2 mM TCEP at 37 °C for 1 h and analyzed by MALDI-MS.

Purification of recombinant haSMase

Recombinant haSMase (bc-haSMase) was expressed in SF21 cells using the baculovirus expression vector system [16]. Unless stated otherwise all chromatographic steps were carried out at 4 °C and all buffers contained dialyzable octyl-β-D-glucopyranoside (OG) as detergent and 0.02% (w/v) NaN_3 as preservative.

$(NH_4)_2SO_4$ precipitation. After addition of 0.1% (w/v) Nonidet P-40, 0.1 mM $ZnCl_2$ and 0.02% (w/v) NaN_3, the expression supernatant was subjected to 60% $(NH_4)_2SO_4$ precipitation and stirred overnight at 4 °C. After ultracentrifugation (235 000 ***g***, 30 min, 4 °C), the precipitate was dissolved in 220 mL of concanavalin A buffer (30 mM Tris/HCl, pH 7.2, 0.5 M NaCl, 0.2% (w/v) OG, 1 mM each of $CaCl_2$, $MgCl_2$ and $MnCl_2$, 0.1 mM $ZnCl_2$).

Concanavalin A-Sepharose chromatography. After additional ultracentrifugation (235 000 ***g***, 30 min, 4 °C) and filtration (0.2 μm), the protein solution was applied to a concanavalin A Sepharose column (1.6 × 10 cm, 0.5 mL·min^{-1}) equilibrated with 10 column volumes of concanavalin A buffer. After washing with 10 column volumes of concanavalin A buffer (1 mL·min^{-1}), bound glycoproteins were eluted at room temperature in reverse direction with a linear gradient of 0–20% (w/v) methyl-α-D-mannopyranoside in concanavalin A buffer (2 × 4.5 column volumes, 1 mL·min^{-1}) followed by 4.5 column volumes of 20% (w/v) methyl-α-D-mannopyranoside in concanavalin A buffer.

Octyl-Sepharose chromatography. Fractions of the concanavalin A eluate with the highest specific haSMase activity were pooled and loaded onto an Octyl-Sepharose column (1.6 × 10 cm, 0.5 mL·min^{-1}) equilibrated with 10 column volumes of Octyl-Sepharose buffer (30 mM Tris/HCl, pH 7.2). After washing with 10 column volumes of Octyl-Sepharose buffer, elution was performed at room temperature in reverse direction using 7.5 column volumes of Octyl-Sepharose buffer containing 1% (w/v) OG (1 mL·min^{-1}).

Anion exchange chromatography. Combined fractions of the Octyl-Sepharose eluate with the highest specific haSMase activity were concentrated (2 mg protein·mL^{-1}) and buffer was exchanged for DEAE buffer A [50 mM Tris/HCl, pH 7.6, 0.4% (w/v) OG] using ultrafiltration concentrators (Centricon-50, Amicon). A Fractogel EMD DEAE column (1 × 1 cm) equilibrated in DEAE buffer A was loaded with the Octyl-Sepharose eluate (2–3 mg protein per column) and washed with 15 mL of DEAE buffer A (0.75 mL·min^{-1}). After neutralization, fractions of the flowthrough containing haSMase activity were concentrated (1.5 mg enzyme·mL^{-1}) in Centricon-50 and buffer was exchanged for 25 mM NH_4HCO_3, 0.1% (w/v) OG. The purified enzyme was frozen in liquid N_2 and stored at −80 °C.

Purification of haSMase from human placenta

Homogenization, $(NH_4)_2SO_4$ precipitation and chromatography on concanavalin A-Sepharose, Octyl-Sepharose and Matrex Gel Red A were performed as described previously [6]. The detergent Nonidet P-40 was replaced by dialyzable OG during Matrex Gel Red A chromatography.

Anion exchange chromatography. Combined fractions of the Matrex Gel Red A eluate with the highest specific haSMase activity were concentrated (2 mL) and buffer was exchanged for DEAE buffer B [50 mM Tris/HCl, pH 7.6, 0.2% (w/v) OG] using Centricon-50 (Amicon). A Fractogel EMD DEAE column (1 × 2 cm) equilibrated in DEAE buffer B was loaded with the Matrex Gel Red A eluate and washed with 20 mL of DEAE buffer B (1 mL·min^{-1}). Fractions of the flowthrough with haSMase activity were concentrated in Centricon-50 (0.5 mL) and buffer was exchanged for 20 mM Tris/HCl, pH 7.2, 0.1% (w/v) OG. The enzyme was frozen and stored at −80 °C.

RP-HPLC purification. RP-HPLC separation of the remaining proteins was performed on a SMART System (Pharmacia, Uppsala, Sweden) using a Nucleosil C4 column (5 μm particle size, 300 Å pore, 2 × 100 mm) at a flow rate of 100 μL·min^{-1}. Trifluoroacetic acid (0.1%) in water was used as eluent A, 0.06% trifluoroacetic acid in 70% acetonitrile and 30% isopropanol as eluent B. The lyophilized DEAE fractions were dissolved in 200 μL 6 M guanidine-HCl and applied to the C4 column equilibrated in 30% B. After washing with 30% B for 20 min, proteins were eluted with a linear gradient of 30–75% B in 40 min. Fractions containing purified pl-haSMase were identified by

SDS/PAGE and MALDI-MS analysis. After adding 0.04% (w/v) OG, the organic solvent was removed at room temperature in a vacuum system. For tryptic digestion lyophilized pl-haSMase was dissolved in 25 mM NH_4HCO_3 containing 10% acetonitrile.

Acid sphingomyelinase and protein assay

ASMase activity was measured using [^{3}H]SM as substrate in the presence of Nonidet P-40 [2]. Protein was quantified by the BCA-method [17] with bovine serum albumin as standard.

Results

Identification of four disulfide bonds

Recombinant haSMase (bc-haSMase) was expressed in SF21 cells using the baculovirus expression vector system [16] and purified to apparent homogeneity as judged by SDS/PAGE analysis (not shown). The purified enzyme had a specific activity of ≈ 0.8 mmol·mg^{-1}·h^{-1} in a detergent containing assay system [2]. The sequence of mature bc-haSMase contains 23 additional N-terminal amino acid residues compared to the sequence of native haSMase from human placenta. Its N-terminus is His60 referring to the open reading frame of the haSMase-cDNA [16]. As native haSMase, the recombinant enzyme contains 17 cysteines and six potential N-glycosylation sites.

For disulfide bond analysis, pure bc-haSMase was subjected to tryptic digestion and the resulting peptides were analyzed by MALDI-MS. Figure 1 shows the complete amino acid sequence of mature bc-haSMase presented as theoretical tryptic peptides T1 to T43. The MALDI-MS spectra of the tryptic digest of bc-haSMase without prior treatment (A) and after reduction with tris(2-carboxyethyl) phosphine (TCEP) (B) are shown in Fig. 2. Table 1 lists the theoretical and experimental masses of identified peptides. Four signals at m/z 1976.2, 2815.8, 3355.0 and 3991.1 were detected only in the MALDI-MS spectrum of the untreated tryptic digest of bc-haSMase (Fig. 2A). They all correspond to the calculated masses of disulfide linked peptides, namely T41 + T42, T27 + T30, T10 + T11 and T14 + T17 (Table 1). The occurrence of the first three disulfide-linked peptides directly indicates the existence of the disulfide bonds C594-C607 (T41 + T42), C385-C431 (T27 + T30) and C120-C131 (T10 + T11). The corresponding non-bridged peptides T41, T27, T30 and T11 appeared in the MALDI-MS spectrum of the reduced tryptic digest (Fig. 2B). The mass of peptide T41 (1146.3 Da) is nearly

Fig. 1. Amino acid sequence of mature recombinant haSMase expressed in SF21 cells using the baculovirus expression system and of native haSMase from human placenta. The theoretical tryptic peptides T1-T43 of the recombinant enzyme (N-terminus: His60) and T1p-T39p of placental haSMase (N-terminus: Gly83) are shown. Cysteines (red) and potential N-glycosylation sites (blue) are marked with boldface. The N-terminal amino acid residues His60 and Gly83 are underlined.

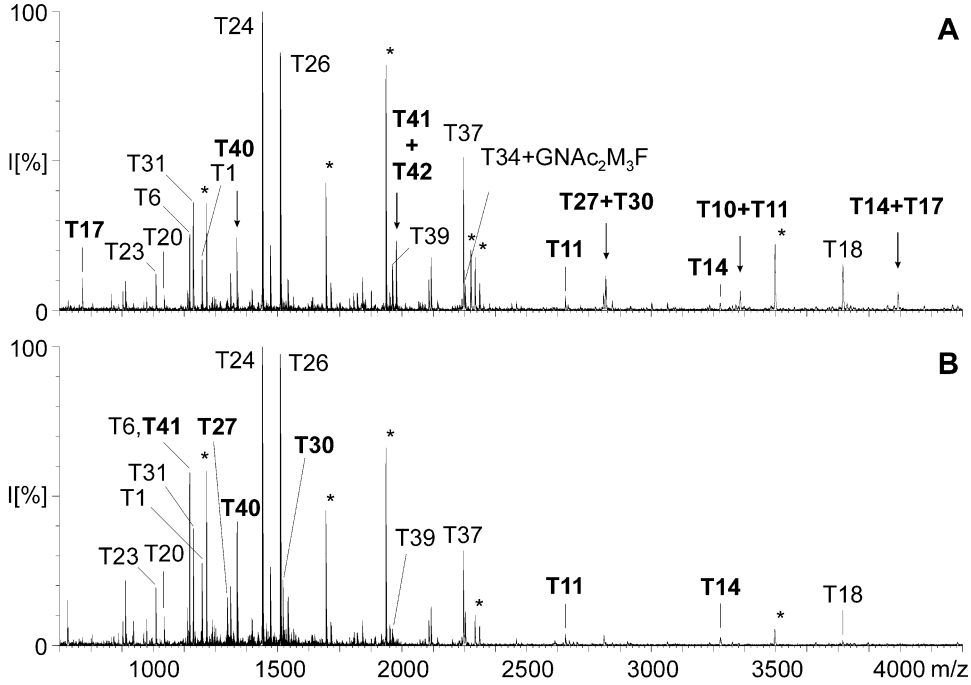

Fig. 2. MALDI mass spectra of the tryptic digest of bc-haSMase before (A) and after reduction with TCEP (B). The spectra were acquired in reflectron mode using α-cyano-4-hydroxycinnamic acid as matrix. Signals assigned to theoretical tryptic peptides are labeled according to Fig. 1. Cystine- and cysteine-containing peptides are marked with boldface and the positions of disulfide-linked peptides are indicated by arrows. Signals of nontryptic peptides or peptides resulting from RP- or KP-cleavage are marked by an asterisk. Matrix suppression: below 700 Da. I, relative intensity.

Table 1. Theoretical and experimental masses of identified tryptic peptides of the tryptic digest of bc-haSMase before and after reduction with TCEP. Cysteine- and cystine-containing peptides are marked with boldface. Monoisotopic masses of the MH^+ ions were measured in the reflectron mode. Mass accuracy is in the range of 500 p.p.m. CHO: carbohydrate side chain $Man3(GlcNAc)_2Fuc$. Masses are given in Da.

	Before reduction		After reduction	
Peptide	MH^+ theoretical	MH^+ experimental	MH^+ theoretical	MH^+ experimental
T17	716.4	716.2	716.4	716.2
T23	1011.5	1011.3	1011.5	1011.4
T20	1044.6	1044.5	1044.6	1044.5
T41	1146.3	–	1146.3	(1146.6)
T6	1146.7	1146.5	1146.7	1146.6
T31	1161.5	1161.3	1161.5	1161.5
T1	1196.3	1196.5	1196.3	1196.4
T34 + CHO	2253.0	2253.0	2253.0	2253.0
T27	1297.6	–	1297.6	1297.6
T40	1335.6	1335.5	1337.6 [b]	1337.7 [b]
T24	1438.8	1438.8	1438.8	1438.8
T26	1510.8	1510.9	1510.8	1510.9
T30	1520.9	–	1520.9	1521.0
T39	1960.9	1961.1	1960.9	1961.1
T41 + T42	1976.0	1976.2		
T37	2245.1	2245.3	2245.1	2245.3
T11	2654.3	2654.6	2654.3	2654.4
T27 + T30	2815.5	2815.8		
T14	3276.4	–	3276.4	3276.7
T10 + T11	3354.7	3355.0		
T18	3769.2 [a]	3769.4 [a]	3769.2 [a]	3768.9 [a]
T14 + T17	3990.5 [a]	3991.1 [a]		

[a] Average mass. [b] T40 reduced.

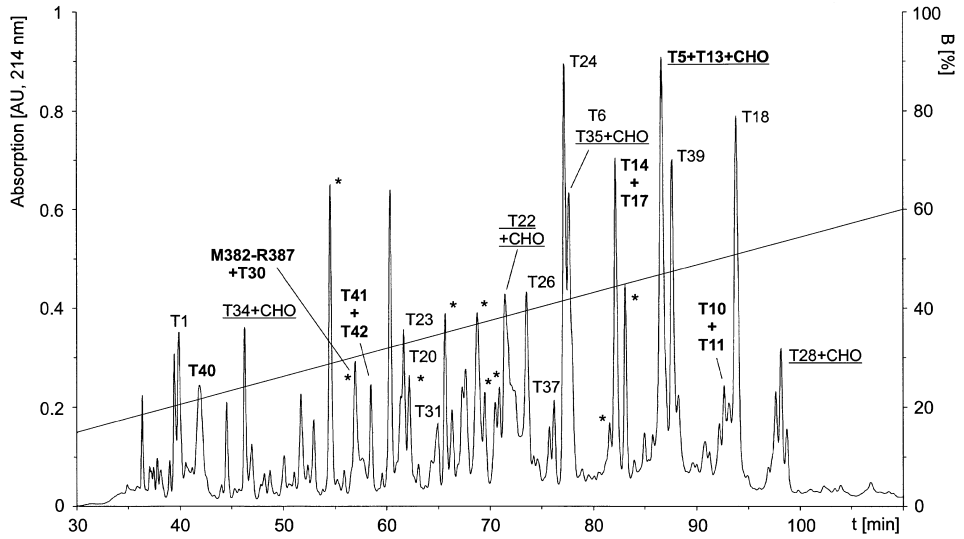

Fig. 3. RP-HPLC separation of the peptides from tryptic digestion of bc-haSMase. Peptides were separated on a Vertex Nucleosil C18 column. Trifluoroacetic acid (0.1%) in water was used as eluent A, 0.06% trifluoroacetic acid in 70% acetonitrile, 30% isopropanol as eluent B. Peptides were eluted with a linear gradient of 15% to 60% B in 80 min. Signals assigned to tryptic peptides are labeled according to Fig. 2. Disulfide-linked peptides are marked with boldface and glycopeptides are underlined (CHO: carbohydrate side chain). Signals of nontryptic peptides or peptides resulting from RP- or KP-cleavage are marked by an asterisk.

identical with that of peptide T6 (1146.7 Da). A clear assignment of the signal at 1146.6 Da (Table 1B) was achieved by peptide separation and PSD analysis.

The signal at m/z 3991.1, corresponding to the calculated mass of T14 + T17 does not allow the direct assignment of a disulfide bond, as T14 contains three cysteines (C221, C226 and C227). For the assignment of the exact location of the disulfide bonds, a further analysis was necessary. One additional disulfide bond was identified by a 2-Da mass shift of peptide T40 after reduction (Table 1), which indicates the existence of an internal disulfide bond between the two cysteines in this peptide (C584 and C588).

In order to confirm the above results and to localize the residual disulfide bonds, the peptides of the untreated tryptic digest of bc-haSMase were isolated by reversed-phase HPLC (Fig. 3) and subjected to MALDI-MS analysis. Table 2 shows the theoretical and experimental masses of the isolated disulfide-linked peptides T40, T10 + T11, T41 + T42 and M382-R387 + T30. Reduction of peptide T40 resulted in a mass shift of 2 Da to 1337.5 Da and alkylation with iodacetamide increased the mass by 114 Da to 1451.7 Da. In the cases of T10 + T11, T41 + T42 and M382-R387 + T30 the signals of the disulfide-linked peptides disappeared on reduction and the masses of the composing peptides were detected (Table 2). The reduced peptides show a 57-Da mass shift on alkylation with iodacetamide. These results prove the existence of the four disulfide bridges

Table 2. Theoretical and experimental masses of the isolated disulfide-linked peptides T40, T41 + T42, T10 + T11 and M382-R387 + T30 of bc-haSMase without prior treatment, after reduction with TCEP, and after reduction and alkylation with iodacetamide. Monoisotopic masses of the MH^+ ions were measured in the reflectron mode. Mass accuracy is in the range of 500 p.p.m.

Peptide	MH^+ theoretical (Da)	MH^+ experimental (Da)	Treatment
T40	1335.6	1335.6	–
T40	1337.6	1337.5	Reduction
T40 + 2 iodacetamide	1451.6	1451.7	Reduction + alkylation
T41 + T42	1976.0	1975.9	–
T41	1146.6	1146.5	Reduction
T42	832.4	832.3	Reduction
T41 + iodacetamide	1203.7	1203.7	Reduction + alkylation
T42 + iodacetamide	889.4	889.4	Reduction + alkylation
T10 + T11	3354.7	3354.6	–
T10	703.4	703.5	Reduction
T11	2654.3	2654.3	Reduction
M382-R387 + T30	2275.1	2275.2	–
M382-R387	757.3	757.3	Reduction
T30	1520.9	1520.9	Reduction
M382-R387 + iodacetamide	814.3	814.4	Reduction + alkylation
T30 + iodacetamide	1577.9	1577.9	Reduction + alkylation

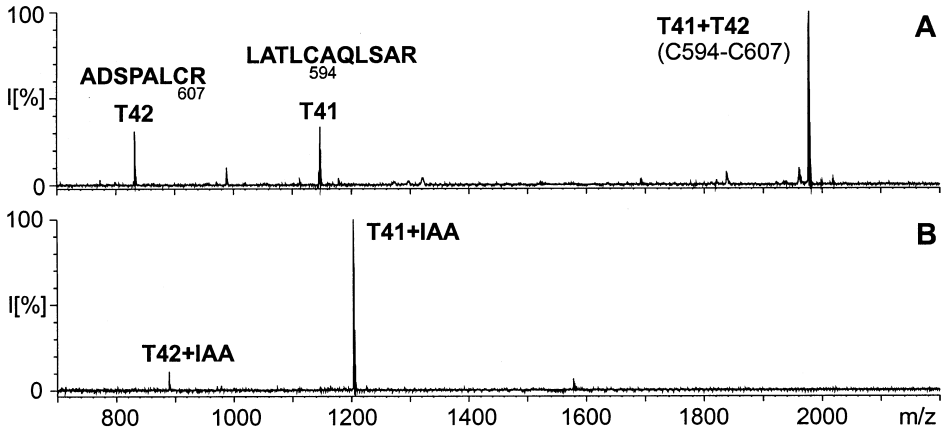

Fig. 4. MALDI mass spectra of the isolated disulfide-linked peptide T41 + T42 without prior treatment (A) and after reduction with TCEP and alkylation with iodacetamide (B). The sequences of the peptides T41 and T42 are shown. The spectra were acquired in reflectron mode using α-cyano-4-hydroxycinnamic acid as matrix. Matrix suppression: below 600 Da. I, relative intensity.

C120-C131 (T10 + T11), C584-C588 (T40), C594-C607 (T41 + T42) and C385-C431 (M382-R387 + T30). Figure 4 shows the MALDI-MS spectra of the disulfide-linked peptide T41 + T42 without prior treatment (A) and after reduction with TCEP and subsequent alkylation with iodacetamide (B). Figure 4A shows the signal of the disulfide-linked peptide as well as the masses of its composing peptides. This results from on-target or gas phase cleavage of the S-S bond [18] and confirm the above results.

Identification of nontryptic peptides

MALDI-MS analysis of the tryptic digest of bc-haSMase showed several intensive signals of unknown origin (Fig. 2). For identification, these peptides were isolated and sequenced by PSD. Their sequences correspond to haSMase sequences as shown in Table 3, thus excluding contaminations. They possess at least one terminus that resulted from nontryptic cleavage, presumably due to a contamination of trypsin by chymotrypsin [19].

Unexpectedly, the disulfide-linked peptide T27 + T30 (Fig. 2A) was not found in any of the RP-HPLC fractions. Instead, a peptide with a mass of 2275.1 Da was isolated. MALDI-MS and PSD analysis with and without prior reduction revealed that this peptide consists of a nontryptic peptide M382-R387 (C385), linked to peptide T30 (C431), thus proving the existence of the C385-C431 disulfide bond (Table 2).

The appearance of the peptides P239-K249, P475-R496, Y446-R474 and H609-R625 instead of the expected peptides T16, T33 and T43 may be due to the drastic digestion conditions (high trypsin concentration, long incubation time) used to generate tryptic peptides in sufficient yield. Tryptic RP- and KP-cleavage sites are often selectively missed due to the low rate of hydrolysis of these cleavage sites (e.g. both KP-cleavage sites in peptide T13, Fig. 1). Cleavage of peptide T43 between R625 and P626 indicates the existence of a C-terminal peptide P626-C629. Due to its low molecular mass this peptide could not be detected. The ambiguity of the signal at m/z 1214.5, which corresponds to the calculated mass of peptide T34 (N503), was resolved by PSD analysis, which showed that cleavage between R238 and P239 resulted in a peptide P239-K249 with the same mass.

Table 3. Theoretical and experimental masses of identified nontryptic peptides after tryptic digestion of bc-haSMase. Monoisotopic masses of the MH^+ ions were measured in the reflectron mode. Mass accuracy is in the range of 500 p.p.m. T + sequence: peptides, which result from RP- or KP-cleavage; nT + sequence: nontryptic peptides.

Peptide	MH^+ theoretical (Da)	MH^+ experimental (Da)	Identification by
T P239-K249	1214.6	1214.5	Mass, PSD
nT L481-R496	1693.9	1694.0	Mass, PSD
nT E541-N555	1713.8	1713.7	Mass, PSD
nT W275-R289	1818.9	1818.8	Mass, PSD
T H609-R625	1934.0	1934.2	Mass, PSD
nT T458-R474	2115.9	2115.9	Mass, PSD
nT N381-S386 + T30	2233.1	2233.4	Mass, reduction
nT M382-R387 + T30	2275.1	2275.2	Mass, reduction, PSD
T P475-R496	2292.2	2292.5	Mass, PSD
nT G456-R474	2310.0	2309.8	Mass, PSD
T Y446-R474	3494.6	3494.9	Mass

Glycosylation analysis – identification of a peptide with two disulfide bonds

RP-HPLC of the peptides of the tryptic bc-haSMase digest led to the isolation of a very hydrophobic peptide with a mass of 8960.5 Da (Fig. 5A, Table 4). Treatment with PNGase F reduced its mass to the calculated mass of a disulfide-linked peptide T5 + T13 (Fig. 5B). Its signal disappeared on reduction and the masses of the free peptides T5 and T13 were detected (Fig. 5C). Treatment of peptide T5 + T13 (4 Cys) with iodacetamide did not result in a mass shift. These results prove that peptide T5 (C89 and C92) is linked with peptide T13 (C157 and C165) by two disulfide bonds arranged either C89-C157 and C92-C165 or C89-C165 and C92-C157. The definite localization of these bonds was complicated by the absence of proteolytic cleavage sites between C89 and C92, as well as between C157 and C165 and by the extreme hydrophobicity of peptide T5 + T13. As these disulfide bonds are part of the highly conserved SAP-domain of haSMase [13], we assume that the arrangement of the disulfide bonds is analogous to that found in SAP B-D [14,15]. We have proved this for the disulfide bond C120-C131. For the remaining cysteines, the arrangement that follows from the homology is C89-C165 and C92-C157.

The glycosylation of T5 (N86) and T13 (N175) was calculated from the mass difference between the glycosylated peptide and the deglycosylated peptide (Table 4). Carbohydrate structures were suggested in accordance to known N-glycosylation structures [20]. We conclude that both peptides possess a fucosylated N-glycan of the type $GlcNAc_2Man_3Fuc$. Four additional peptides containing one potential N-glycosylation site each were isolated by RP-HPLC: T22 (N335), T28 (N395), T34 (N503) and T35 (N520). MALDI-MS analysis of these peptides before and after treatment with PNGase F revealed that positions N335, N395 and N503 bear fucosylated N-glycans of the type $GlcNAc_2Man_3Fuc$. Position N520 contains the nonfucosylated core structure $GlcNAc_2Man_3$. These results demonstrate that all six potential N-glycosylation sites of bc-haSMase are glycosylated.

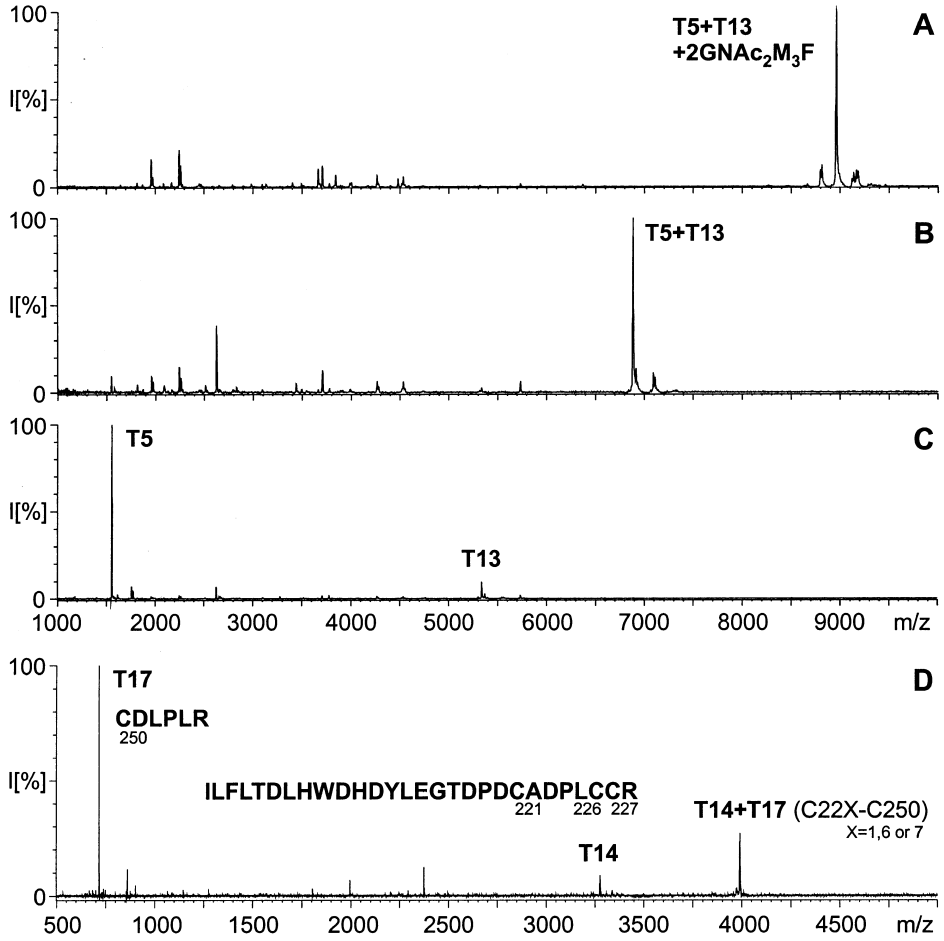

Fig. 5. MALDI mass spectra of the isolated disulfide-linked peptides T5 + T13 and T14 + T17. Without prior treatment of T5 + T13 (A) and T14 + T17 (D), after deglycosylation of peptide T5 + T13 with PNGase F (B) and after subsequent reduction with TCEP (C). The spectra were acquired in linear mode using sinapinic acid (A–C) or in reflectron mode using α-cyano-4-hydroxycinnamic acid as matrix (D). Matrix suppression: 1000 Da (A–C), 600 Da (D). I: relative intensity.

Table 4. Theoretical and experimental masses of the isolated disulfide-linked peptides T14 + T17 and T5 + T13 of bc-haSMase without prior treatment and after reduction with TCEP. Peptide T5 + T13 was reduced with and without prior treatment with PNGase F. Monoisotopic masses of the MH^+ ions were measured in the reflectron mode, average masses in the linear mode. Mass accuracy is in the range of 500 p.p.m. GNAc, N-acetyl-glucosamine; M, mannose; F, fucose.

Peptide	MH^+ theoretical (Da)	MH^+ experimental (Da)	Treatment
T14 + T17	3987.8	3988.1	–
T14	3276.4	3276.4	Reduction
T17	716.4	716.2	Reduction
T5 + T13 + $2GNAc_2M_3F$	8961.9*	8960.5*	–
T5 + T13	6886.0*	6885.7*	Deglycosylation
T5 + $GNAc_2M_3F$	2592.8*	2592.4*	Reduction
T13 + $GNAc_2M_3F$	6374.1*	6374.5*	Reduction
T5	1553.7	1553.7	Deglycosylation + reduction
T13	5336.2*	5336.3*	Deglycosylation + reduction

*Average mass.

Identification of two disulfide bonds including C226 and C227

The disulfide-linked peptide T14 + T17 (4 Cys) discussed above was isolated by RP-HPLC. MALDI-MS analysis of this peptide revealed a total mass of 3988.1 Da (Fig. 5D, Table 4), indicating that the four cysteines are arranged in two disulfide linkages. This was confirmed by the failure to alkylate peptide T14 + T17 with iodacetamide. As there is no protease, which can cleave between adjacent cysteines, a chemical method [21] was used to analyze the two disulfide bonds in peptide T14 + T17. This method allows discrimination of cysteines in close vicinity, including adjacent cysteines. It employs partial reduction of peptides or proteins possessing at least two disulfide bonds by TCEP at pH 3 followed by cyanylation of the nascent sulfhydryl groups by 1-cyano-4-dimethylamino-pyridinium tetrafluoroborate. The partially reduced and cyanylated peptides are isolated by RP-HPLC and subjected to cleavage on the N-terminal side of cyanylated cysteines in aqueous ammonia and subsequent reduction of the remaining disulfide bonds. The masses of the specific fragments obtained for each partially reduced isomer reveal the location of the disulfide bridge opened by the limited reduction.

After partial reduction of peptide T14 + T17 followed by cyanylation, the resulting peptides were separated by RP-HPLC (Fig. 6). Species 1 corresponds to a singly cyanylated peptide T14 containing an internal disulfide bond. Compared to species 1, only a low amount of species 2 was obtained. Probably species 2 represents a partially reduced peptide lacking the disulfide bond within peptide T14. MALDI-MS analysis of the fragmented and reduced species 1 showed one intensive signal at *m/z* 3016.2 (not shown), which corresponds to fragment I201-C226 and indicates cyanylation and cleavage at C227. Without prior reduction the same signal appeared 2 Da lower at m/z 3014.3, thus indicating the existence of a disulfide bond between C221 and C226 of T14. Therefore, C250 (T17) is linked with C227 (T14), forming the second disulfide linkage of peptide T14 + T17. The monoisotopic mass of peptide I201-C226 appeared one dalton below its calculated mass. This results from partial amidation of its C-terminus formed by cleavage of the parent peptide in 1 M NH_4OH [22].

The existence of a C221-C226 disulfide bond was confirmed by PSD analysis of the fragment I201-C226 with and without prior reduction (Fig. 7). As PSD-fragmentation preferentially occurs at the N-terminal peptide bond of prolines [23], b23 should be a major fragment of the reduced peptide I201-C226. After reduction the PSD spectrum of

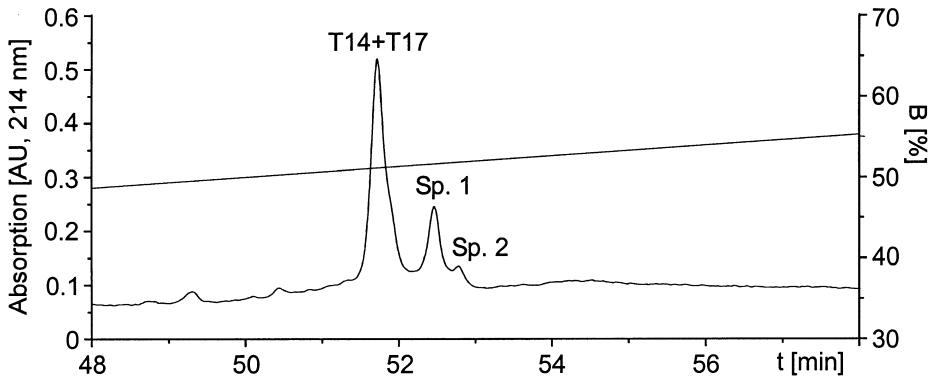

Fig. 6. RP-HPLC separation of partially reduced and cyanylated peptides of peptide T14 + T17. Trifluoroacetic acid (0.1%) in water was used as solvent A, 0.08% trifluoroacetic acid in 80% acetonitrile, 20% water as solvent B. Peptide separation was achieved on a Vertex Nucleosil C18 column using a linear acetonitrile-gradient of 30% to 70% B in 60 min. Sp. 1, 2: species 1, 2.

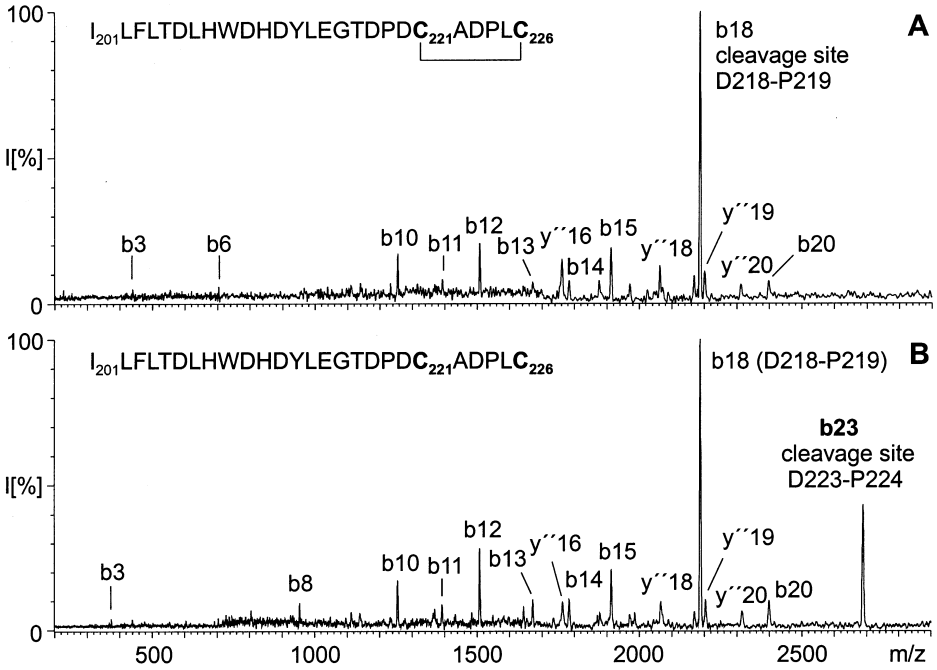

Fig. 7. PSD spectra of fragment I201-C226 before (A) and after reduction with TCEP (B). Fragment I201-C226 resulting from cleavage on the N-terminal side of Cys227 was selected by ion gating with and without prior reduction and analyzed by PSD-sequencing. PSD-fragments were detected by reducing the reflectron voltage in 12 steps. The individual scans were stitched and the stitched spectra are displayed. Fragment b23 (m/z 2687.9, cleavage between Asp223 and Pro224) is marked with boldface. I: relative intensity.

peptide I201-C226 shows an intensive signal at *m/z* 2687.9 corresponding to fragment b23, which appears only in the absence of a C221-C226 disulfide bond. This proves the presence of the C221-C226 disulfide bond. The appearance of the signals of fragments y″16, y″18, y″19 and y″20 2 Da below the masses of their reduced forms support the above results.

Analysis of the disulfide bonds of haSMase from human placenta

In order to confirm that the disulfide bond pattern obtained for the recombinant protein is physiological, haSMase was purified from human placenta (pl-haSMase) and digested by trypsin (Fig. 1, theoretical tryptic peptides T1p-T39p). In the MALDI-MS spectrum five signals at m/z 1335.6 (T36), 1976.1 (T37 + T38), 2815.6 (T23 + T26), 3355.1 (T6 + T7), and 3990.2 (T10 + T13) were detected (Fig. 8) that disappeared on reduction, giving rise to the composing peptides (Table 5). This proves the existence of the four disulfide bridges C120-C131 (T6 + T7), C385-C431 (T23 + T26), C584-C588 (T36), and C594-C607 (T37 + T38). For the recombinant peptide T14 + T17, we identified a 1–2, 3–4 disulfide pattern, suggesting that the corresponding placental peptide T10 + T13 has the same disulfide linkages in these positions (C221-C226,

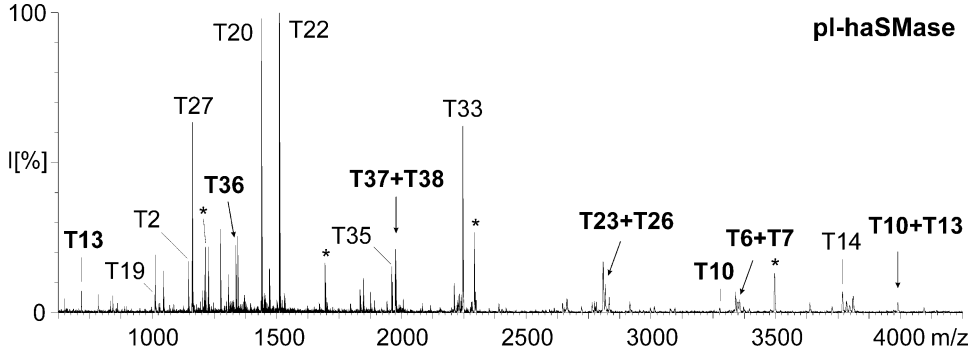

Fig. 8. MALDI mass spectrum of the tryptic digest of native haSMase from human placenta. The spectrum was acquired in reflectron mode using α-cyano-4-hydroxycinnamic acid as matrix. Signals assigned to tryptic peptides are labeled according to Fig. 1. Cystine- and cysteine-containing peptides are marked with boldface and the positions of disulfide-linked peptides are indicated by arrows. Signals of nontryptic peptides or peptides resulting from RP- or KP-cleavage are marked by an asterisk. Matrix suppression: below 700 Da. I, relative intensity.

Table 5. Calculated and measured masses of identified disulfide-linked peptides of the tryptic digest of placental haSMase before and after reduction with TCEP. Monoisotopic masses of the MH^+ ions were measured in the reflectron mode. Mass accuracy is in the range of 500 p.p.m. Masses are given in Da.

	Before reduction		After reduction	
Peptide	MH^+ theoretical	MH^+ experimental	MH^+ theoretical	MH^+ experimental
T38	832.4	832.5	832.4	–
T37	1146.3	–	1146.3	(1146.6)
T23	1297.6	–	1297.6	1297.7
T36	1335.6	1335.6	1337.6 [b]	1337.6 [b]
T26	1520.9	–	1520.9	1520.9
T37 + T38	1976.0	1976.1		
T7	2654.3	–	2654.3	2654.4
T23 + T26	2815.5	2815.6		
T10	3276.4	–	3276.4	3277.1
T6 + T7	3354.7	3355.1		
T10 + T13	3990.5 [a]	3990.2 [a]		

[a] Average mass. [b] T36 reduced.

C227-C250). A signal that corresponds to a glycosylated disulfide-linked peptide T1 + T9 (similar to peptide T5 + T13 of bc-haSMase) could not be detected, possibly because the remaining cysteines may have been part of nontryptic peptides. However, the disulfide bridges that we have determined for placental haSMase so far are completely identical with those of the recombinant enzyme. We therefore conclude that placental and recombinant haSMase possess an identical disulfide bond structure.

Discussion

In recent years functional recombinant haSMase has been produced in different eukaryotic expression systems [16,24]. Despite these advances, only limited information about its structural properties or post-translational modifications has become available so far. Here, we have investigated the disulfide bond structure of haSMase by MALDI mass spectrometry. The identified disulfide bond pattern of haSMase with a proposed domain structure is presented in Fig. 9. In recombinant bc-haSMase expressed in SF21 cells we determined eight disulfide bonds, six of which were also definitely identified in the native human protein. This structural information is essential for further analysis of functional domains of the enzyme and conclusive structure predictions by molecular modeling.

The high degree of sequence homology between the SAPs and the N-terminal region of haSMase (C89-C165) led to the hypothesis that haSMase possesses an intramolecular SAP-type activator domain [13]. The disulfide bond

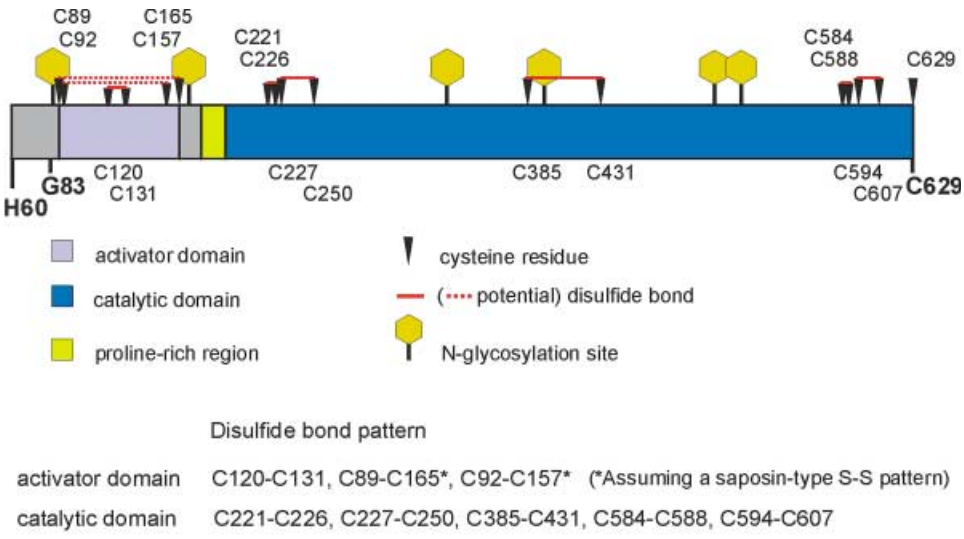

Fig. 9. Disulfide bond pattern and domain structure of haSMase. The identified disulfide bond structure of haSMase is presented. The N-terminus of native haSMase from human placenta is Gly83 [6] referring to the open reading frame of the haSMase-cDNA (His60: N-terminus of mature bc-haSMase expressed in SF21 cells using the baculovirus expression vector system [16]). Contrary to position N503 in the native human protein [7], glycosylation site N503 of bc-haSMase is glycosylated.

arrangement of SAP B-D has been analyzed in recent years by a combination of enzymatic and chemical cleavage and mass spectrometry and was found to be identical in these three proteins [14,15]. This high degree of structural homology led to the assumption that the six conserved cysteine residues of the haSMase SAP-domain are arranged in the identical pattern (C120-C131, C89-C165 and C92-C157). The activator domain hypothesis is supported by the identification of a disulfide bond between C120 and C131 (Fig. 9). In addition, identification of the glycosylated disulfide-linked peptide (D80-K93) + (S149-R200) proves that C89 and C92 are linked with C157 and C165 by two disulfide bonds, most likely in the SAP-type pattern C89-C165 and C92-C157. This shows that the six cysteines of the haSMase SAP-domain are arranged in three internal disulfide bridges, forming a closed disulfide bond structure.

In this report we describe, for the first time, the complete determination of the disulfide bridges in the presumed catalytic C-terminal domain of haSMase (Fig. 9). This domain contains 11 cysteines, 10 of which are arranged in five disulfide bonds. The existence of the three disulfide linkages C385-C431, C584-C588 and C594-C607 was proved by MALDI-MS analysis of enzymatically cleaved bc-haSMase. Analysis of the remaining disulfide bonds required a strategy, which allows discrimination between the adjacent cysteines C226 and C227. Identification of the two disulfide bonds C221-C226 and C227-C250 was achieved by a combination of a method of partial reduction, which was shown to be capable of discriminating cysteines in close vicinity [21] and MALDI-PSD analysis. The importance of the disulfide bond structure for the enzymatic activity of haSMase is underlined by the fact that substitution of Cys157 to Arg within the postulated SAP-type activator domain renders the enzyme inactive [25]. This demonstrates that the N-terminal SAP-domain of haSMase is essential for the catalytic activity of the enzyme.

We showed by MALDI-MS analysis of the isolated glycopeptides that all glycosylation sites of bc-haSMase are used. In the positions N1–5 we detected fucosylated N-glycans of the type $GlcNAc_2Man_3Fuc$ and in the position N6 we found the nonfucosylated core structure $GlcNAc_2Man_3$. The lack of glycosylation at N503 in the native human protein [7] is the most significant difference in glycosylation between recombinant and native haSMase. Differences in the carbohydrate processing in human and insect cells have been reported previously [6,16]. In contrast to the recombinant protein, placental haSMase possesses mainly high mannose and/or hybrid type N-glycans. Because the specific activity of both enzymes is nearly identical, we conclude that the differences in glycosylation do not affect the active site or have a significant influence on the structure of the protein.

Structural analysis was markedly complicated by the hydrophobicity of many of the disulfide-linked peptides. Due to the high hydrophobicity of peptide T5 + T13 of the SAP-type domain, several attempts to analyze the arrangement of its two disulfide bonds by partial reduction were unsuccessful, as separation of the partially reduced isomers by RP-HPLC was not possible. Another difficulty was the appearance of several nontryptic cleavage products, which may be due to a contamination of trypsin by chymotrypsin [19]. Even though varying digestion conditions were used, generation of these peptides could not be suppressed. However, the existence of the C385-C431 disulfide bond could be proved by identification of the nontryptic disulfide-linked peptide M382-R387 + T30 by PSD analysis. PSD sequencing of a 1934.2-Da peptide revealed the sequence H609-R625, thus proving cleavage of the C-terminal peptide T43 (C629) between R625 and P626. Due to its low molecular mass, a peptide P626-C629 could not be detected. Considering the fact that all other 16 cysteines of haSMase are involved in disulfide bridges, it can be concluded that the C-terminal C629, if it is part of the sequence of the enzyme, must be unbridged.

Irrespective of their relative arrangement, the two outer disulfide bonds of the activator domain form clamps around the C120-C131 disulfide bond, spanning large sequences of more than 60 amino acids (Fig. 9), similar to the conserved disulfide bond pattern of SAP A-D [14,15]. One function of the SAP-type disulfide pattern may be the formation of a compact tertiary structure, necessary for stabilization of saposin-type lysosomal proteins against the aggressive conditions in the lysosomes. This is supported by the demonstration that loss of disulfide bridges in SAP B leads to an increased susceptibility of the protein to proteolytic attack [26]. Contrary to the disulfide bonds of the SAP-domain, the five disulfide bridges of the C-terminal catalytic portion of haSMase are arranged sequentially, forming a 7–8, 9–10, etc., pattern. The linear arrangement of disulfide bridges near the active site may facilitate proteolytic attack on the catalytic region. This could be one explanation for the observed rapid loss of the enzymatic activity of lysosomal haSMase in the presence of tricyclic antidepressants, such as desipramine [27].

In summary, this report presents the complex disulfide bond structure (eight bridges) of haSMase. The disulfide bridges that we have identified in placental haSMase completely correspond to the disulfide pattern found in recombinant bc-haSMase. This indicates that the recombinant and the native human protein possess an identical disulfide bond structure. The knowledge of the disulfide connectivities provides important experimental constraints that can greatly aid the elucidation of the structure of the enzyme by molecular modeling and X-ray crystallography. In addition, this structural information is important for the production of recombinant enzyme for future enzyme replacement therapy trials.

Acknowledgements

This work was supported by grants of the Deutsche Forschungsgemeinschaft (SFB 400) and by the Fonds der Chemischen Industrie.

References

1. Schuchman, E.H. & Desnick, R.J. (1995) Niemann–Pick disease types A and B: Acid sphingomyelinase deficiencies. In *The Metabolic and Molecular Bases of Inherited Disease*, 7th edn. (Scriver, C.R., Beaudet, A.L., Sly, W.S. & Valle, D., eds), pp. 2601–2624. McGraw Hill, New York.
2. Quintern, L.E., Weitz, G., Nehrkorn, H., Tager, J.M., Schram, A.W. & Sandhoff, K. (1987) Acid sphingomyelinase from human urine: purification and characterization. *Biochim. Biophys. Acta* **922**, 323–336.

3. Quintern, L.E., Schuchman, E.H., Levran, O., Suchi, M., Ferlinz, K., Reinke, H., Sandhoff, K. & Desnick, R.J. (1989) Isolation of cDNA clones encoding human acid sphingomyelinase: occurrence of alternatively processed transcripts. *EMBO J.* **8**, 2469–2473.
4. Schuchman, E.H., Suchi, M., Takahashi, T., Sandhoff, K. & Desnick, R.J. (1991) Human acid sphingomyelinase. Isolation, nucleotide sequence and expression of the full-length and alternatively spliced cDNAs. *J. Biol. Chem.* **266**, 8531–8539.
5. Hurwitz, R., Ferlinz, K., Vielhaber, G. & Sandhoff, K. (1994) Processing of human acid sphingomyelinase in normal and I-cell fibroblasts. *J. Biol. Chem.* **269**, 5440–5445.
6. Lansmann, S., Ferlinz, K., Hurwitz, R., Bartelsen, O., Glombitza, G. & Sandhoff, K. (1996) Purification of acid sphingomyelinase from human placenta: Characterization and N-terminal sequence. *FEBS Lett.* **399**, 227–231.
7. Ferlinz, K., Hurwitz, R., Mozcall, H., Lansmann, S., Schuchman, E.A. & Sandhoff, K. (1997) Functional characterization of the N-glycosylation sites of human acid sphingomyelinase by site directed mutagenesis. *Eur. J. Biochem.* **243**, 511–517.
8. Spiegel, S., Foster, D. & Kolesnick, R. (1996) Signal transduction through lipid second messengers. *Curr. Opin. Cell Biol.* **8**, 159–167.
9. Hannun, Y.A. (1996) Functions of ceramide in coordinating cellular responses to stress. *Science* **274**, 1855–1859.
10. Huwiler, A., Kolter, T., Pfeilschifter, J. & Sandhoff, K. (2000) Physiology and pathophysiology of sphingolipid metabolism and signaling. *Biochim. Biophys. Acta* **1485**, 63–99.
11. Kirschnek, S., Paris, F., Weller, M., Grassme, H., Ferlinz, K., Riehle, A., Fuks, Z., Kolesnick, R. & Gulbins, E. (2000) CD95-mediated apoptosis *in vivo* involves acid sphingomyelinase. *J. Biol. Chem.* **275**, 27316–27323.
12. Klein, A., Henseler, M., Klein, C., Suzuki, K., Harzer, K. & Sandhoff, K. (1994) Sphingolipid activator protein (sap-D) stimulates the lysosomal degradation of ceramide *in vivo*. *Biochem. Biophys. Res. Com.* **200**, 1440–1448.
13. Ponting, C.P. (1994) Acid sphingomyelinase posesses a domain homologous to its activator proteins: saposins B and D. *Protein Sci.* **3**, 359–361.
14. Vaccaro, A.M., Savioli, R., Barca, A., Tatti, M., Ciaffoni, F., Maras, B., Siciliano, R., Zappacosta, F., Amoresano, A. & Pucci, P. (1995) Structural analysis of saposin C and B. Complete localization of disulfide bridges. *J. Biol. Chem.* **270**, 9953–9960.
15. Tatti, M., Salvioli, R., Ciaffoni, F., Pucci, P., Andolfo, A., Amoresano, A. & Vaccaro, A.M. (1999) Structural and membrane-binding properties of saposin D. *Eur. J. Biochem.* **263**, 486–494.
16. Bartelsen, O., Lansmann, S., Nettersheim, M., Lemm, T., Ferlinz, K. & Sandhoff, K. (1998) Expression of recombinant human acid sphingomyelinase in insect *Sf*21 cells: purification, processing and enzymatic characterization. *J. Biotechnol.* **63**, 29–40.
17. Smith, P.K., Krohn, R.I., Hermanson, G.T., Mallia, A.K., Gartner, F.H., Provenzano, M.D., Fujimoto, E.K., Goeke, N.M., Olson, B.J. & Klenk, D.C. (1985) Measurement of protein using bicinchoninic acid. *Anal. Biochem.* **150**, 76–85.
18. Patterson, S.D. & Katta, V. (1994) Prompt fragmentation of disulfide-linked peptides during matrix-assisted laser desorption ionization mass spectrometry. *Anal. Chem.* **66**, 3727–3732.
19. O'Dowd, B.F., Cumming, D.A., Gravel, R.A. & Mahuran, D. (1988) Oligosaccharide structure and amino acid sequence of the major glycopeptides of mature human beta-hexosaminidase. *Biochemistry* **27**, 5216–5226.
20. Kornfeld, R. & Kornfeld, S. (1985) Assembly of asparagine-linked oligosaccharides. *Annu. Rev. Biochem.* **54**, 631–664.
21. Wu, J. & Watson, J.T. (1997) A novel methodology for assignment of disulfide bond pairings in proteins. *Protein Sci.* **6**, 391–398.
22. Schuette, C.G., Lemm, T., Glombitza, G.J. & Sandhoff, K. (1998) Complete localization of disulfide bonds in GM2 activator protein. *Protein Sci.* **7**, 1039–1045.
23. Kaufmann, R., Hirsch, D. & Sprengler, B. (1994) Sequencing of peptides in a time-of-flight mass spectrometer: Evaluation of post source decay following matrix-assisted laser desorption ionization (MALDI). *Int. J. Mass Spectrom. Ion Proc.* **86**, 137–154.
24. He, X., Miranda, S.R., Xiong, X., Dagan, A., Gatt, S. & Schuchman, E.H. (1999) Characterization of human acid sphingomyelinase purified from the media of overexpressing Chinese hamster ovary cells. *Biochim. Biophys. Acta* **1432**, 251–264.
25. Ida, H., Rennert, O.M., Eto, Y. & Chan, W.Y. (1993) Cloning of a human acid sphingomyelinase cDNA with a new mutation that renders the enzyme inactive. *J. Biochem.* **114**, 15–20.
26. Faull, K.F., Higginson, J., Waring, A.J., Johnson, J., To, T., Whitelegge, J.P., Stevens, R.L., Fluharty, C.B. & Fluharty, A.L. (2000) Disulfide connectivity in cerebroside sulfate activator is not necessary for biological activity or alpha-helical content but is necessary for trypsin resistance and strong ligand binding. *Arch. Biochem. Biophys.* **376**, 266–274.
27. Hurwitz, R., Ferlinz, K. & Sandhoff, K. (1994) The tricyclic antidepressant desipramine causes proteolytic degradation of lysosomal sphingomyelinase in human fibroblasts. *Biol. Chem. Hoppe Seyler* **375**, 447–450.